Contemporary Mathematics
http://ojs.wiserpub.com/index.php/CM/

Research Article

Painlevé Analysis and Chiral Solitons from Quantum Hall Effect

Nikolay A. Kudryashov[1], Anjan Biswas[2,3,4], Qin Zhou[5], Yakup Yildirim[6,7,8]*

[1]Department of Applied Mathematics, National Research Nuclear University MEPhI (Moscow Engineering Physics Institute), 31 Kashirskoe Shosse, 115409 Moscow, Russian Federation
[2]Department of Mathematics and Physics, Grambling State University, Grambling, LA 71245-2715, USA
[3]Department of Applied Sciences, Cross-Border Faculty of Humanities, Economics and Engineering, University of Galati, Galati-800201, Romania
[4]Department of Mathematics and Applied Mathematics, Sefako Makgatho Health Sciences University, Medunsa-0204, South Africa
[5]School of Mathematical and Physical Sciences, Wuhan Textile University, Wuhan, China
[6]Department of Computer Engineering, Biruni University, Istanbul-34010, Turkey
[7]Mathematics Research Center, Near East University, 99138 Nicosia, Cyprus
[8]Faculty of Arts and Sciences, University of Kyrenia, 99320 Kyrenia, Cyprus
E-mail: yyildirim@biruni.edu.tr

Received: 15 July 2024; **Revised:** 17 August 2024; **Accepted:** 10 October 2024

Abstract: This study examines the generalized Schrödinger equation governing chiral solitons. We assess its integrability using the Painlevé test for nonlinear partial differential equations. Our analysis shows that the equation fails the Painlevé test, suggesting the Cauchy problem cannot be solved using the inverse scattering transform. However, through a traveling wave reduction, we find that the resulting nonlinear ordinary differential equation does satisfy the Painlevé test. Therefore, we establish a general solution for this reduced equation, which we outline accordingly.

***Keywords*:** generalized Schödinger equation, chiral soliton, Painlevé test, traveling wave solution, first integral

MSC: 81V70

1. Introduction

The exploration of chiral solitons arising from quantum Hall effects has been ongoing for several decades. One significant class of gauge theoretical models, initially investigated by Jackiw and Pi [1–4], describes non-relativistic matter coupled to a Chern-Simons gauge field. This framework provides a straightforward approach to understanding non-relativistic interacting anyons and supports the existence of unidirectional chiral solitons [5–8]. These solitons play a crucial role in the quantum Hall effect, where chiral excitations are observed to manifest prominently.

We delve into the chiral nonlinear Schrödinger equation, exploring its integrability through a comprehensive Painlevé analysis. Subsequently, we unveil soliton solutions derived from this model, detailing both the Painlevé test methodology and the extraction process of soliton solutions using the traveling wave hypothesis. The analytical intricacies are thoroughly elucidated throughout the ensuing sections of this paper.

DOI: https://doi.org/10.37256/cm.5420245313

1.1 *Governing model*

The equation representing chiral solitons is formulated as

$$i q_t + \frac{1}{2} q_{xx} + i\lambda \left(q q_x^* - q^* q_x\right) q = 0. \tag{1}$$

Eq. (1) was first identified in paper [3] as describing anyons and chiral solitons on a line. Numerous investigations of this equation have been conducted in the literature (see, for instance [9–34]). An intriguing characteristic of this equation is its possession of four conservation laws [9]. The modified Euler equations were rediscovered in the semiclassical limit of the one-dimensional Schrödinger equation in a study documented in paper [35]. Soliton solutions of Eq. (1) have been extensively examined in papers [36, 37], employing specialized techniques for constructing exact solutions.

In this paper, we utilize the Painlevé test to assess the integrability of Eq. (1). Indeed, we can assert with near absolute certainty that Eq. (1) does not fall into the category of integrable partial differential equations. This conclusion is supported by our knowledge of a limited number of second-order nonlinear partial differential equations, similar to Eq. (1), that are integrable via the inverse scattering transform. One notable example is the Kaup-Newell equation, which is expressed as follows:

$$i q_t = q_{xx} + i \left(2 b q q_x^* + b q^* q_x\right) q = 0. \tag{2}$$

Another integrable equation derived via the inverse scattering transform is presented in the paper [38], taking the form

$$i q = q_{xx} + i \left(a q q_x^* + b q^* q_x\right) q + \frac{1}{4} b (2b - a) q^3 {q^*}^2 = 0. \tag{3}$$

Taking into account Eqs. (2) and (3), it is expected that Eq. (1) does not pass the Painlevé test, thereby rendering the Cauchy problem associated with Eq. (1) unsolvable using the inverse scattering transform. However, in this paper, we examine the Painlevé property of Eq. (1) and demonstrate that it does not satisfy the necessary condition for integrability among nonlinear partial differential equations (NLPDEs). Furthermore, by applying the Painlevé test for nonlinear partial differential equations, we derive conditions under which a reduction of the partial differential equation can allow it to pass the Painlevé test as a nonlinear ordinary differential equation (NLODE). Subsequently, we demonstrate that such reductions of Eq. (1) to NLODEs do indeed pass the Painlevé test.

Using the traveling wave reduction of Eq. (1), we derive a corresponding nonlinear ordinary differential equation (NLODE) and present its general solution.

The organization of this paper is as follows. Section 2 applies the Painlevé test to the NLPDE (1), showing it does not allow for a solution through the inverse scattering transform in the general case. Sections 3 and 4 detail the Painlevé test applied to the corresponding NLODE derived from Eq. (1). Section 5 covers the general solution derived from the traveling wave reduction of Eq. (1).

2. Painlevé test to Eq. (1)

The Painlevé property is a critical criterion for determining integrability in equations. To explore whether Eq. (1) meets this criterion, we address the Painlevé test via the Kruskal variable, following the methodology detailed in references [38–40]. Initially, we seek a solution to Eq. (1) in this format:

$$q(x,\ t) = u(x,\ t)\, e^{i v(x,\ t)}, \tag{4}$$

where $v(x,\ t)$ and $u(x,\ t)$ denote newly introduced functions. By substituting (4) into Eq. (1), we derive the imaginary and real components of Eq. (1) as shown

$$u_t + u_x v_x + \frac{1}{2} u v_{xx} = 0, \tag{5}$$

and

$$\frac{1}{2} u_{xx} - u v_t - \frac{1}{2} u v_x^2 + 2\lambda u^3 v_x = 0. \tag{6}$$

To conduct the Painlevé test on the system of equations (5) and (6), we proceed with three sequential steps [41–44]. Initially, we substitute the expressions

$$u(x,\ t) = a_0(t) F(x,\ t)^p, \quad v(x,\ t) = b_0(t) F(x,\ t)^r, \tag{7}$$

where $a_0(t)$, $b_0(t)$, and $F(x,\ t)$ represent newly defined functions, and p and r denote powers, we substitute them into the equations derived from the leading terms of the system (5) and (6), which are formulated as

$$u_t + u_x v_x + \frac{1}{2} u v_{xx} = 0, \tag{8}$$

$$\frac{1}{2} u_{xx} + 2\lambda u^3 v_x = 0. \tag{9}$$

Consequently, through these substitutions, we obtain the powers $p = -1$ and $= 1$, along with functions $B_0(t)$ and $a_0(t)$, expressed as follows:

$$a_0(t)^{(1,\ 2)} = \pm \frac{1}{\sqrt{-2\lambda \psi_t}}, \qquad b_0(t) = \psi_t. \tag{10}$$

Our objective is to determine the Fuchs indices, which can take on any form as representations specific to the local solutions $U(x,\ t)$ and $V(x,\ t)$. To accomplish this, we incorporate the following expressions

$$u(x,\ t) = \pm \frac{1}{\sqrt{-2\lambda \psi_t F(x,\ t)}} + a_j F(x,\ t)^{j-1}, \tag{11}$$

$$v(x,\ t) = \psi_t F(x,\ t) + b_j F(x,\ t)^{j+1}, \tag{12}$$

into the system of equations (8) and (9). The Fuchs indices are found from the algebraic equation

$$\det(\mathbf{A}) = 0, \qquad \mathbf{A} = \begin{pmatrix} a_{11} & a_{12} \\ a_{21} & a_{22} \end{pmatrix}, \tag{13}$$

where the matrix elements a_{11} and a_{21} are coefficients at a_j of Eqs. (8), (9) and the matrix elements a_{12} and a_{22} are coefficients at b_j of of Eqs. (8), (9). These coefficients can be written as follows

$$\begin{gathered} a_{11} = 0, \quad a_{12} = \frac{\sqrt{2} F^{j-2} (j^2 - j - 2)}{4 \sqrt{-\lambda \, \psi_t}}, \\ a_{21} = \frac{F^{j-3} (j^2 - 3j - 4)}{2}, \quad a_{22} = \frac{\sqrt{2} F^{j-3} (j+1)}{2 \, \psi_t \sqrt{-\lambda \, \psi_t}}. \end{gathered} \tag{14}$$

By computing $\det \mathbf{A}$, we derive the algebraic equation used to determine the Fuchs indices in this manner:

$$Q(j) = (j+1)^2 (j-2)(j-4). \tag{15}$$

Upon solving Eq. (15), the resulting Fuchs indices are as follows:

$$j_{1,\,2} = -1, \quad j_3 = 2, \quad j_4 = 4. \tag{16}$$

In the third step, we need to verify the arbitrary constants present in the expansions of the solutions for the system of equations (24) and (25). To achieve this goal, we substitute the expansions

$$u(x,\,t) = \sum_{j=0}^{4} a_j(t) F(x,\,t)^{j-1}, \quad v(x,\,t) = \sum_{j=0}^{4} b_j(t) F(x,\,t)^{j+1}, \tag{17}$$

into equations (24) and (25) to determine the arbitrary functions. Following the approach by Kruskal M, we hypothesize that the expression for $F(x,\,t)$ is as follows:

$$F(x,\,t) = x - \psi(t), \tag{18}$$

where $\psi(t)$ represents an arbitrary function.

By inserting (17) into Eqs. (24) and (25), and setting the coefficients of $F(x,\,t)$ to zero at various powers, we derive:

$$b_1 = \frac{\psi_{tt}}{2\,\psi_t}, \qquad a_1 = -\frac{\sqrt{2}\,\psi_{tt}}{6\,\psi_t^2\,\sqrt{-\lambda\,\psi_t}},$$
$$b_2 = \frac{1}{6}\,\psi_t^3 + \sqrt{2}\,a_2(t)\,\psi_t\,\sqrt{-\lambda\,\psi_t} + \frac{2}{9}\,\frac{\psi_{tt}^2}{\psi_t^3}. \tag{19}$$

However, to select an arbitrary function, instead of equality to zero, we get the expression

$$K_2[\psi] = \frac{\sqrt{2}\,(\psi_t\,\psi_{ttt} - 3\,\psi_{tt}^2)}{6\,\psi_t^3\,\sqrt{-\lambda\,\psi_t}}. \tag{20}$$

This indicates that Eq. (1) does not satisfy the Painlevé test for NLPDEs, and the Cauchy problem associated with this equation cannot be solved by the inverse scattering transform. Nonetheless, it is evident that there exists solutions for $\psi(t)$ of equation:

$$\psi_t\,\psi_{ttt} - 3\,\psi_{tt}^2 = 0. \tag{21}$$

These solutions of Eq. (21) enable the application of reductions to Eq. (1), potentially revealing its Painlevé property. These specific scenarios will be further examined in the following sections.

One of the solutions to Eq. (21) is as follows:

$$\psi(t) = M_1 + \sqrt{M_1 + M_2\,(t - M_3)}, \tag{22}$$

where M_1, M_2, and M_3 are arbitrary constants. Another solution is $\psi(t) = C_0\,t$, which enables us to seek traveling wave solutions of Eq. (1).

3. Painlevé test for the NLODE associated with Eq. (1)

The utilization of the Painlevé test in NLODEs is now widely recognized. Initially, we derive the NLODE from Eq. (1) via the traveling wave reduction method [45–52]. We seek solutions in the following form:

$$q(x,\,t) = y(z)\,e^{i\,\phi(z)}, \quad z = x - C_0\,t, \tag{23}$$

Here, C_0 represents a wave velocity, while $\phi(z)$ and $y(z)$ denote new functions.

Substituting (23) into Equation (1), we obtain:

$$\frac{1}{2}\,\phi_{zz}\,y + \phi_z\,y_z - C_0\,y_z = 0, \tag{24}$$

and

$$\frac{1}{2}\,y_{zz}-\phi_z^2\,y-2\,\lambda\,\phi_z\,y^2+C_0\,\phi_z\,y=0. \tag{25}$$

Eqs. (24) and (25) can be written taking a new variable $\varphi(z)=\phi_z$ as the following

$$\frac{1}{2}\,\varphi_z\,y+\varphi\,y_z-C_0\,y_z=0, \tag{26}$$

and

$$\frac{1}{2}\,y_{zz}-\varphi^2\,y-2\,\lambda\,\varphi\,y^2+C_0\,\varphi\,y=0. \tag{27}$$

System of equations (26) and (27) is also studied using the three steps by the algorithm of the Painlevé test. Taking into account that the Eqs. (26) and (27) are autonomous we can use in the first step the formulas

$$y=a_0\,z^p,\quad \varphi=b_0\,z^r, \tag{28}$$

In this context, p and r denote the orders of poles for solutions $y(z)$ and $\varphi(z)$. By substituting (28) into the equations, we derive the equation with the leading terms, which are presented as:

$$\frac{1}{2}\,\varphi_z\,y+\varphi\,y_z-C_0\,y_z=0, \tag{29}$$

and

$$\frac{1}{2}\,y_{zz}-2\,\lambda\,\varphi\,y^2=0. \tag{30}$$

The branches of solutions are derived from the system of equations (29) and (30) as follows

$$\left(a_0^{(1,\,2)},\,-1\right)=\left(\pm\,(2\,\lambda\,C_0)^{-\frac{1}{2}},\,-1\right),\qquad (b_0,\,r)=(C_0,\,0)\,. \tag{31}$$

We utilize the following formulas in the second step to compute the Fuchs indices

$$y=\pm\frac{a_0^{(1,\,2)}}{z}+a_j\,z^{j-1},\quad \varphi=b_0+b_j\,z^j. \tag{32}$$

Substituting (32) into equations involving the leading elements (29) and (30), we derive the equation that characterizes the Fuchs indices as follows:

$$Q(j) = (j^2 - 3j - 4)(j - 2) = 0. \tag{33}$$

From solving Eq. (33), we derive the Fuchs indices:

$$j_1 = -1, \quad j_2 = 2, \quad j_3 = 4. \tag{34}$$

Next, we examine the arbitrary coefficients in the local solutions $y(z)$ and $u(z)$. This is achieved by substituting the following expansions into Eqs. (26) and (27).

$$y = \pm \frac{1}{\sqrt{2\lambda C_0}\, z} + a_1 + a_2 z + a_3 z^2 + a_4 z^3 + \ldots, \tag{35}$$

$$\varphi = C_0 + b_1 z + b_2 z^2 + b_3 z^3 + b_4 z^4 + \ldots. \tag{36}$$

The coefficients b_2 and a_4, determined by setting expressions at different powers of z to zero, are found to be arbitrary functions of t, while the remaining coefficients in the expansions are structured accordingly.

$$b_1 = 0, \quad b_3 = 0, \quad b_4 = -\frac{b_2(C_0^3 - 2b_2)}{3C_0}, \tag{37}$$

$$a_1 = 0, \quad a_2 = -\frac{\sqrt{2}\lambda\,(C_0^3 - 2b_2)}{12\,(C_0\lambda)^3}, \quad a_3 = 0. \tag{38}$$

Finally expansions (35) and (36) can be written as follows

$$y = \pm \frac{1}{\sqrt{2\lambda C_0}\,(z - z_0)} - \frac{\sqrt{2}\lambda\,(C_0^3 - 2b_2)}{12\,(C_0\lambda)^3}(z - z_0) + a_4 (z - z_0)^3 + \ldots, \tag{39}$$

$$\phi_z = C_0 + b_2\,(z - z_0)^2 - \frac{b_2(C_0^3 - 2b_2)}{3C_0}\,(z - z_0)^4 + \ldots. \tag{40}$$

The expansions (39) and (40) clearly indicate the presence of three arbitrary constants: z_0, b_2, and a_4. Thus, Eq. (1) satisfies the Painlevé test and the necessary conditions for solving the Cauchy problem associated with NLODEs (24) and (25). The next section will explore the general solution of these equations.

4. Painlevé test for the self-similar solutions associated with Eq. (1)

Solution (22) indicates that the system of equations (5) and (6) possesses self-similar solutions in the form

$$u(x,\, t) = t^{-\frac{1}{4}}\, f(z), \qquad v(x,\, t) = g(z), \qquad z = \frac{x}{\sqrt{t}}. \tag{41}$$

These variables allow us to obtain a non-autonomous second-order ordinary differential equation for $f(z)$ in the form

$$f_{zz} + 2\lambda\, z f^3 + \left(4\lambda\, \mu + \frac{z^2}{4}\right) f - \frac{\mu^2}{f^3} = 0, \tag{42}$$

where μ is an arbitrary constant.

Applying the Painlevé test to Eq. (42), we find that there are integer Fuchs indices given by:

$$j_1 = -1, \quad j_2 = 4. \tag{43}$$

However, by substituting

$$f(z) = \sum_{j=0}^{4} a_j\, (z - z_0)^{j-1} \tag{44}$$

in the third step of the Painlevé test for Eq. (42), we obtain

$$\begin{aligned} & a_0^{(1,\,2)} = \pm \frac{1}{\sqrt{\lambda\, z_0}}, \quad a_1 = -\frac{(\lambda\, z_0)^{5/2}}{3\lambda^3 z_0^4}, \quad a_2 = -\frac{(\lambda\, z_0)^{5/2}\,(48\lambda\, \mu\, z_0^2 - 3z_0^4 - 16)}{72\lambda^3 z_0^5}, \\ & a_3 = -\frac{(\lambda\, z_0)^{5/2}\,(728\lambda\, \mu\, z_0^2 + 9z_0^4 - 28)}{108\lambda^3 z_0^6}. \end{aligned} \tag{45}$$

However, we cannot consider a_4 as an arbitrary coefficient in the Laurent series expansion. Consequently, the necessary condition for the existence of the general solution of Eq. (42) is not fulfilled.

5. Traveling wave solutions of Eq. (1)

We explore the general solution to the NLODE derived from Eq. (1). The system described by equations (24) and (25) is structured as:

$$\frac{1}{2}\,\phi_{zz}\, y + \phi_z\, y_z - C_0\, y_z = 0, \tag{46}$$

and

$$\frac{1}{2}y_{zz}-\phi_z^2\,y-2\lambda\,\phi_z\,y^2+C_0\,\phi_z\,y=0. \tag{47}$$

Written in terms of its first integral, Eq. (46) appears as:

$$y^2\,\phi_z-C_0\,y^2=C_1, \tag{48}$$

Here, C_1 represents an integration constant. One can note that the constant of integration corresponds to the arbitrary constant b_2.

Substituting ϕ_z from (48) into Eq. (47), we obtain the following equation after integration

$$y_z^2-2\lambda\,C_0\,y^4+(C_0^2-4\lambda\,C_1)\,y^2+\frac{C_1^2}{y^2}+C_2=0, \tag{49}$$

Here, C_2 represents an integration constant associated with the Fuchs index $j_3=4$.

Consider a new variable

$$y(z)=\sqrt{V(z)}. \tag{50}$$

Written in the form of Eq. (49), it appears as:

$$V_z^2-8\lambda\,C_0\,V^3+(4C_0^2-16\lambda\,C_1)\,V^2+4C_2\,V+4C_1^2=0. \tag{51}$$

Eq. (51) can be solved by employing elliptic functions, which were originally formulated by Weierstrass K and Jacobi G.

With V_1, V_2, and V_3 assumed as real roots of the polynomial equation represented by

$$V^3-\frac{(C_0^2-4\lambda\,C_1)}{2\lambda\,C_0}\,V^2-\frac{C_2}{2\lambda\,C_0}\,V-\frac{C_1^2}{2\lambda\,C_0}=0. \tag{52}$$

We believe that $(V_1\geq V_2\geq V_3)$ and we have the following conditions

$$\begin{aligned}
&V_1\,V_2\,V_3=\frac{C_1^2}{2\lambda\,C_0},\\
&V_1\,V_2+V_1\,V_3+V_2\,V_3=-\frac{C_2}{2\lambda\,C_0},\\
&V_1+V_2+V_3=\frac{(C_0^2-4\lambda\,C_1)}{2\lambda\,C_0}.
\end{aligned} \tag{53}$$

The solution $V(z)$ corresponding to Eq. (51) is given by the following expression

$$V(z) = V_1 - (V_1 - V_2)\,\mathrm{sn}^2\left\{\sqrt{\frac{V_1 - V_3}{8\lambda C_0}}\,(z - z_0);\ S\right\}, \tag{54}$$

where z_0 is a arbitrary constant and S^2 is expressed by formula

$$S^2 = \frac{V_1 - V_2}{V_1 - V_3}. \tag{55}$$

Using the identity

$$\mathrm{sn}^2(z) + \mathrm{cn}^2(z) = 1, \tag{56}$$

the solution to Equation (49) is expressed in this form

$$y(z) = \left[V_2 + (V_1 - V_2)\,\mathrm{cn}^2\left\{\sqrt{\frac{V_1 - V_3}{8\lambda C_0}}\,(z - z_0);\ S\right\}\right]^{\frac{1}{2}}. \tag{57}$$

The solution to Equation (1) can be determined by applying this formula

$$q(x,\ t) = \left[V_2 + (V_1 - V_2)\,\mathrm{cn}^2\left\{\sqrt{\frac{V_1 - V_3}{8\lambda C_0}}\,(x - C_0 t - z_0);\ S\right\}\right]^{\frac{1}{2}} \mathrm{e}^{i\phi(z)}, \tag{58}$$

where $\phi(z)$ is determined by integral

$$\phi(z) = C_3 + C_0 z + C_1 \int \left[V_2 - (V_1 - V_2)\,\mathrm{cn}^2\left\{\sqrt{\frac{V_1 - V_3}{8\lambda C_0}}\,(z - z_0);\ S\right\}\right]^{-1} dz, \tag{59}$$

where C_3 is a arbitrary constant. Solution (57) is a periodic wave.

In the case of $V_1 \geq V_2 = V_3$ we obtain $S = 1$ and the solitary wave solution is expressed by formula

$$q(x,\ t) = \left[V_2 + (V_1 - V_2)\cosh^{-2}\left\{\sqrt{\frac{V_1 - V_2}{8\lambda C_0}}\,(x - C_0 t - z_0)\right\}\right]^{\frac{1}{2}} \mathrm{e}^{i\phi(z)}. \tag{60}$$

Some special solutions can be found from Eqs. (58) and (60).

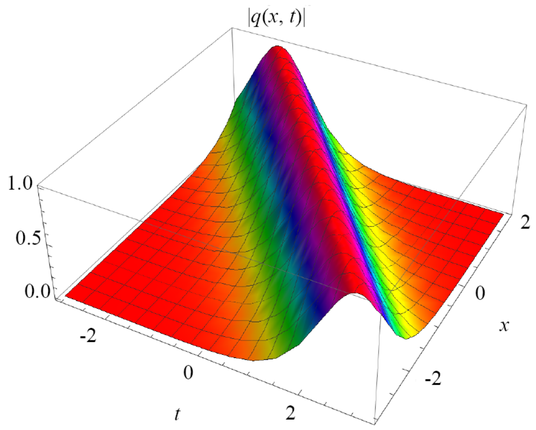

(a) 3D plot

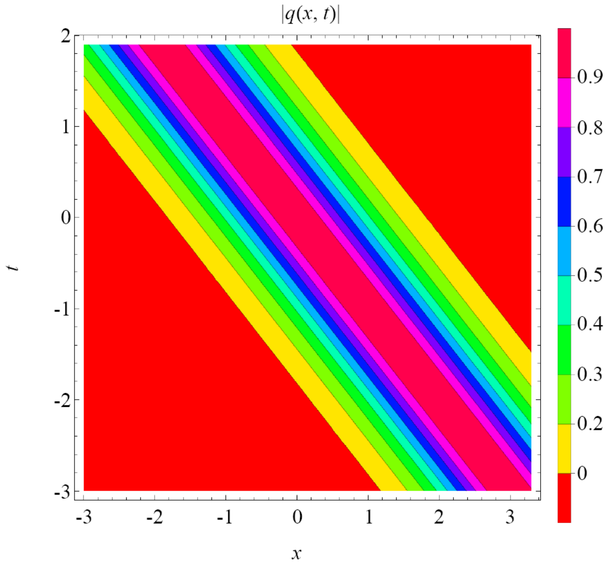

(b) Contour plot

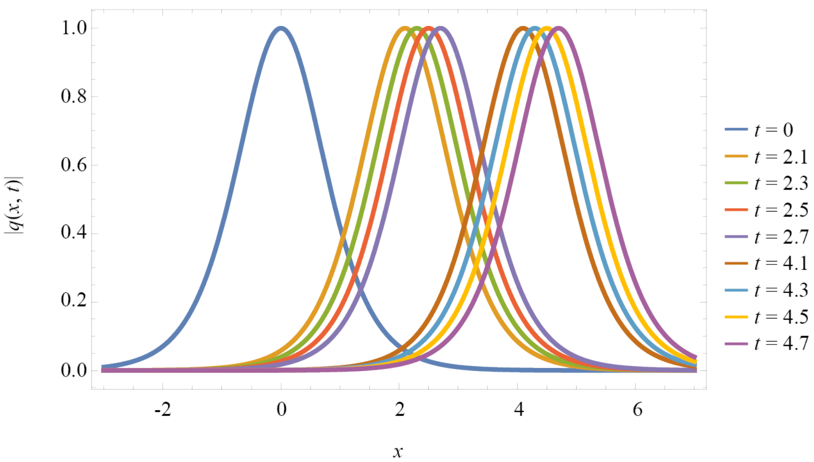

(c) 2D plot

Figure 1. Investigating the distinct properties demonstrated by a bright soliton, alongside the dynamics of its magnitude

Figure 1 presents the characteristics and evolution of the bright soliton solution $q(x, t)$ as described by the complex-valued solution (52). The analysis spans different time instances $t = 0$, 2.1, 2.3, 2.5, 2.7, 4.1, 4.3, 4.5, and 4.7, showcasing the dynamical behavior of the soliton. The specific parameters used for these visualizations include $C_0 = 1$, $C_1 = -1$, $\lambda = 1/4$ and $z_0 = 1$. Figure 1(a) showcases a surface plot of the modulus of the bright soliton solution (52). This plot provides a three-dimensional perspective of the soliton's amplitude over the specified time instances and spatial domain. The surface plot reveals the soliton's profile, highlighting its peak intensity and how it evolves over time. As time progresses, the bright soliton maintains its shape, demonstrating the stability characteristic typical of soliton solutions, despite the changes in the surrounding parameters. Figure 1(b) provides a contour plot of the modulus of the bright soliton solution (52). The contour plot offers a top-down view, emphasizing the soliton's intensity distribution across the spatial and temporal domains. This representation allows for a clearer understanding of the soliton's position and intensity variations at different time instances. The contour lines denote regions of equal intensity, and their spacing and shape indicate the soliton's propagation and interaction with the medium. The contour plot further corroborates the stability and localized nature of the bright soliton, as the contours remain well-defined and concentrated around the soliton peak. Figure 1(c) illustrates a 2D plot of the modulus of the bright soliton solution (52) over time. This plot captures the soliton's amplitude along a specific spatial slice, providing a detailed view of its evolution at discrete time points. The 2D plot reveals how the peak amplitude of the soliton evolves, showing slight modulations due to the parameter settings but overall retaining the soliton's coherent structure. The temporal snapshots indicate the soliton's robustness against dispersive effects and parameter-induced perturbations. Collectively, these subfigures in Figure 1 provide a comprehensive depiction of the bright soliton solution's behavior. The surface plot (Figure 1(a)) illustrates the soliton in a three-dimensional context, emphasizing its spatial-temporal stability. The contour plot (Figure 1(b)) offers a different perspective, focusing on intensity distributions, and the 2D plot (Figure 1(c)) highlights the soliton's temporal evolution. The consistency across these visualizations underscores the inherent stability and robustness of the bright soliton solution under the given parameter regime. This detailed analysis enhances our understanding of the soliton's dynamics and confirms the theoretical predictions of soliton behavior in nonlinear media.

6. Conclusions

This paper investigates the generalized Schrödinger equation for chiral solitons, with a primary focus on determining the integrability of the NLPDE. Two different approaches of the Painlevé test are utilized: one for NLPDEs and another for NLODEs. The findings indicate that the NLPDE does not satisfy the Painlevé test under general conditions. However, by applying a traveling wave reduction, it is shown that the resulting NLODE meets the Painlevé test criteria. As a result, the general solution of the original equation, containing four arbitrary constants, is obtained. Lastly, the results in this article will be expanded, taking into account the previously reported outcomes [53–58].

Conflict of interest

The authors claim that there is no conflict of interest.

References

[1] Jackiw R, Pi SY. Soliton solutions to the gauged nonlinear Schrödinger equation on the plane. *Physical Review Letters*. 1990; 64(25): 2969.

[2] Jackiw R, Pi SY. Time-dependent Chern-Simons solitons and their quantization. *Physical Review D*. 1991; 44(8): 2524.

[3] Aglietti U, Griguolo L, Jackiw R, Pi SY, Seminara D. Anyons and chiral solitons on a line. *Physical Review Letters*. 1996; 77(21): 4406.

[4] Griguolo L, Seminara D. Chiral solitons from dimensional reduction of Chern-Simons gauged non-linear Schrödinger equation: classical and quantum aspects. *Nuclear Physics B*. 1998; 516(1-2): 467-498.

[5] Pashaev OK, Lee JH. Self-dual Chern-Simons solitons and quantum potential. *Journal of Nonlinear Mathematical Physics*. 2001; 8(Suppl 1): 225-229.

[6] Pashaev OK, Lee JH. Chern-Simons solitons in quantum potential. *Chaos, Solitons & Fractals*. 2000; 11(14): 2193-2202.

[7] Martina L, Pashaev OK, Soliani G. Chern-Simons field theory and completely integrable systems. *Physics Letters B*. 1996; 378(1-4): 175-180.

[8] Lee JH, Pashaev O. Chiral solitons in a quantum potential. *Theoretical and Mathematical Physics*. 2009; 160: 986-994.

[9] Biswas A. Perturbation of chiral solitons. *Nuclear Physics B*. 2009; 806(3): 457-461.

[10] Biswas A, Mirzazadeh M, Eslami M. Soliton solution of generalized chiral nonlinear schrodinger's equation with time-dependent coefficients. *Acta Physica Polonica Series B*. 2014; 45(4): 849-866.

[11] Ebadi G, Yildirim A, Biswas A. Chiral solitons with Bohm potential using G'/G method and exp-function method. *Romanian Reports in Physics*. 2012; 64(2): 357-366.

[12] Albosaily S, Mohammed WW, Aiyashi MA, Abdelrahman MA. Exact solutions of the (2 + 1)-dimensional stochastic chiral nonlinear Schrödinger equation. *Symmetry*. 2020; 12(11): 1874.

[13] Slepyan GY, Maksimenko SA, Bass FG, Lakhtakia A. Nonlinear electromagnetics in chiral media: self-action of waves. *Physical Review E*. 1995; 52(1): 1049.

[14] Yang L, Gao B. Solitary wave solution, traveling wave solution and other solutions of variable-coefficients Chiral Schrödinger equation. *International Journal of Geometric Methods in Modern Physics*. 2024; 21(5): 2450100.

[15] Harikumar E, Kumar CN, Sivakumar M. Chiral solitons in a current coupled Schrödinger equation with self-interaction. *Physical Review D*. 1998; 58(10): 107703.

[16] Cheemaa N, Chen S, Seadawy AR. Chiral soliton solutions of perturbed chiral nonlinear Schrödinger equation with its applications in mathematical physics. *International Journal of Modern Physics B*. 2020; 34(31): 2050301.

[17] Ozisik M, Secer A, Bayram M. On the investigation of chiral solitons via modified new Kudryashov method. *International Journal of Geometric Methods in Modern Physics*. 2023; 20(7): 2350117.

[18] Akinyemi L, Inc M, Khater MMA, Rezazadeh H. Dynamical behaviour of Chiral nonlinear Schrödinger equation. *Optical and Quantum Electronics*. 2022; 54(3): 191.

[19] Esen H, Ozdemir N, Secer A, Bayram M, Sulaiman TA, Yusuf A. Solitary wave solutions of chiral nonlinear Schrödinger equations. *Modern Physics Letters B*. 2021; 35(30): 2150472.

[20] Sirisubtawee S, Khansai N, Koonprasert S, Torvattanabun M. Exact solutions of the conformable space-time chiral nonlinear Schrödinger's equations. *Thai Journal of Mathematics*. 2020; Special Issue: 147-166.

[21] Nishino A, Umeno Y, Wadati M. Chiral nonlinear Schrödinger equation. *Chaos, Solitons & Fractals*. 1998; 9(7): 1063-1069.

[22] Primatarowa MT, Stoychev KT, Kamburova RS. Soliton dynamics in chiral molecular chains with first-and third-neighbour interactions. *The European Physical Journal B-Condensed Matter and Complex Systems*. 2002; 29: 291-294.

[23] Biswas A. Chiral solitons in 1 + 2 dimensions. *International Journal of Theoretical Physics*. 2009; 48: 3403-3409.

[24] Vyas VM, Patel P, Panigrahi PK, Kumar CN, Greiner W. Chirped chiral solitons in the nonlinear Schrödinger equation with self-steepening and self-frequency shift. *Physical Review A-Atomic, Molecular, and Optical Physics*. 2008; 78(2): 021803.

[25] Ozisik M, Bayram M, Secer A, Cinar M, Yusuf A, Sulaiman TA. Optical solitons to the (1 + 2)-dimensional Chiral non-linear Schrödinger equation. *Optical and Quantum Electronics*. 2022; 54(9): 558.

[26] Maimistov AI. Completely integrable models of nonlinear optics. *Pramana*. 2001; 57: 953-968.

[27] Pashaev OK, Lee JH. Black holes and solitons of the quantized dispersionless NLS and DNLS equations. *The ANZIAM Journal*. 2002; 44(1): 73-81.

[28] Meradji A, Triki H, Wei C. Chirped periodic and localized waves of the (1 + 2)-dimensional chiral nonlinear Schrödinger equation. *Optik*. 2023; 287: 171046.

[29] Biswas A, Yildirim Y, Yasar E, Zhou Q, Moshokoa SP, Belic M. Chiral solitons with bohm potential by modified simple equation method and trial equation scheme. *Acta Physica Polonica A*. 2018; 134(6): 1120-1125.

[30] Bulut H, Sulaiman TA, Demirdag B. Dynamics of soliton solutions in the chiral nonlinear Schrödinger equations. *Nonlinear Dynamics*. 2018; 91: 1985-1991.

[31] Neirameh A, Eslami M. New optical soliton of stochastic chiral nonlinear Schrödinger equation. *Optical and Quantum Electronics*. 2023; 55(5): 444.

[32] Biswas A. Chiral solitons with time-dependent coefficients. *International Journal of Theoretical Physics*. 2010; 49: 79-83.

[33] Kamyar H, Mohammad M, Kaushik D, Anusmita D, Soheil S. A study of different wave structures of the (2 + 1)-dimensional chiral Schrödinger equation. *Russian Journal of Nonlinear Dynamics*. 2022; 18(2): 231-241.

[34] Chen JL, Dai CQ, Wang XG. Chirped domain wall arrays and solitary waves in a generalized nonlinear Schrödinger equation. *Communications in Theoretical Physics*. 2011; 55(2): 335.

[35] Lee JH, Lin CK, Pashaev OK. Shock waves, chiral solitons and semiclassical limit of one-dimensional anyons. *Chaos, Solitons & Fractals*. 2004; 19(1): 109-128.

[36] Johnpillai AG, Yildirim A, Biswas A. Chiral solitons with Bohm potential by Lie group analysis and traveling wave hypothesis. *Romanian Journal of Physics*. 2012; 57(3-4): 545-554.

[37] Biswas A, Milovic D. Chiral solitons with Bohm potential by He's variational principle. *Physics of Atomic Nuclei*. 2011; 74: 755-757.

[38] Clarkson PA, Cosgrove CM. Painleve analysis of the non-linear Schrodinger family of equations. *Journal of Physics A: Mathematical and General*. 1987; 20(8): 2003.

[39] Weiss J, Tabor M, Carnevale G. The Painlevé property for partial differential equations. *Journal of Mathematical Physics*. 1983; 24(3): 522-526.

[40] Baldwin D, Hereman W. Symbolic software for the Painlevé test of nonlinear ordinary and partial differential equations. *Journal of Nonlinear Mathematical Physics*. 2006; 13(1): 90-110.

[41] Ablowitz MJ, Segur H. Exact linearization of a Painlevé transcendent. *Physical Review Letters*. 1977; 38(20): 1103.

[42] Ablowitz MJ, Ramani A, Segur H. A connection between nonlinear evolution equations and ordinary differential equations of P-type. I. *Journal of Mathematical Physics*. 1980; 21(4): 715-721.

[43] Kudryashov NA. Painlevé analysis and exact solutions of the Korteweg-de Vries equation with a source. *Applied Mathematics Letters*. 2015; 41: 41-45.

[44] Kudryashov NA. Painlevé analysis and exact solutions of the fourth-order equation for description of nonlinear waves. *Communications in Nonlinear Science and Numerical Simulation*. 2015; 28(1-3): 1-9.

[45] Kudryashov NA, Safonova DV, Biswas A. Painlevé analysis and a solution to the traveling wave reduction of the Radhakrishnan-Kundu-Lakshmanan equation. *Regular and Chaotic Dynamics*. 2019; 24: 607-614.

[46] Kudryashov NA, Safonova DV. Painlevé analysis and traveling wave solutions of the fourth-order differential equation for pulse with non-local nonlinearity. *Optik*. 2021; 227: 166019.

[47] Kudryashov NA. Method for finding highly dispersive optical solitons of nonlinear differential equations. *Optik*. 2020; 206: 163550.

[48] Malomed BA. New findings for the old problem: Exact solutions for domain walls in coupled real Ginzburg-Landau equations. *Physics Letters A*. 2022; 422: 127802.

[49] He S, Malomed BA, Mihalache D, Peng X, He Y, Deng D. Propagation dynamics of radially polarized symmetric Airy beams in the fractional Schrödinger equation. *Physics Letters A*. 2021; 404: 127403.

[50] Qiu Y, Malomed BA, Mihalache D, Zhu X, Peng J, He Y. Generation of stable multi-vortex clusters in a dissipative medium with anti-cubic nonlinearity. *Physics Letters A*. 2019; 383(22): 2579-2583.

[51] Malomed BA. Multidimensional dissipative solitons and solitary vortices. *Chaos, Solitons & Fractals*. 2022; 163: 112526.

[52] Susanto H, Malomed BA. Embedded solitons in second-harmonic-generating lattices. *Chaos, Solitons & Fractals*. 2021; 142: 110534.

[53] Hussain A, Parveen T, Younis B, Ahamd HU, Ibrahim T, Sallah M. Dynamical behavior of solitons of the (2 + 1)-dimensional Konopelchenko Dubrovsky system. *Scientific Reports*. 2024; 14(1): 147.

[54] Liu Z, Hussain A, Parveen T, Ibrahim TF, Yousif Karrar OO, Al-Sinan BR. Numerous optical soliton solutions of the Triki-Biswas model arising in optical fiber. *Modern Physics Letters B*. 2024; 38(20): 2450166.

[55] Luo R, Abbas N, Hussain A, Ali S. A new sensitive visualization, solitary wave profiles and conservation laws of ion sound waves arising in plasma. *Optical and Quantum Electronics*. 2024; 56(3): 415.

[56] Chávez-Vázquez S, Lavín-Delgado JE, Gómez-Aguilar JF, Razo-Hernández JR, Etemad S, Rezapour S. Trajectory tracking of Stanford robot manipulator by fractional-order sliding mode control. *Applied Mathematical Modelling*. 2023; 120: 436-462.

[57] Mohammadi H, Kumar S, Rezapour S, Etemad S. A theoretical study of the Caputo-Fabrizio fractional modeling for hearing loss due to Mumps virus with optimal control. *Chaos, Solitons & Fractals*. 2021; 144: 110668.

[58] Baleanu D, Aydogn SM, Mohammadi H, Rezapour S. On modelling of epidemic childhood diseases with the Caputo-Fabrizio derivative by using the Laplace Adomian decomposition method. *Alexandria Engineering Journal*. 2020; 59(5): 3029-3039.